

EVALUATION OF TIME TO DEPTH CONVERSION ALGORITHMS FOR DEPTH VELOCITY MODEL BUILDING

L. da S. Sadala Valente, J.C. Costa, and J. Schleicher

email: *jesse@ufpa.br, js@ime.unicamp.br*

keywords: *Time-to-depth conversion, velocity model building, depth migration, image ray*

ABSTRACT

Time-to-depth conversion of a velocity model is highly desirable to provide alternative initial depth velocity models for tomographic methods. Unfortunately, the problem is intrinsically unstable and thus requires regularization. Recently, a number of similar techniques using dynamic ray tracing along image-rays have been proposed to achieve this aim. We review three time-to-depth conversion techniques, discuss their algorithmic procedures and show their differences by applying them to a 2D synthetic data set. In particular, we demonstrate that the different procedures react differently to different kinds of regularization. Although the image-ray trajectories and the resulting depth velocity models depend on the regularization employed, the final depth images corresponding to these different models are very similar.

INTRODUCTION

Over the years, time migration has been routinely employed for seismic imaging, since it is a very fast and robust process. In part, the reason for the success of time migration is that time velocity-model building is a very well understood process, leading to high-quality migration velocity models in time. Moreover, velocity errors affect the images only locally and much less than in depth migration. More recently, new algorithms for time migration velocity analysis based on prestack time migration (PSTM) are emerging (Fomel, 2003; Schleicher et al., 2008; Schleicher and Costa, 2009). These approaches can be used to obtain a focusing velocity model for PSTM, bypassing the conventional CMP-based velocity analysis.

On the other hand, in areas with complex geological structure, as for instance in the presence of strong lateral velocity variations, seismic depth migration is necessary to obtain a reliable image. This, in turn, requires the availability of a velocity model in depth. For this reason, depth velocity model building is a critical phase for successful depth imaging. Usually, the estimation of a depth velocity model relies on tomographic techniques based on iterative algorithms. Several tomography procedures have been proposed for the estimation of depth velocity models (see, for example, Billette et al., 2003; Clapp et al., 2004).

Often, tomographic methods ignore previously available time-migration velocity models and start all over again from constant background velocities or a constant vertical gradient. More sophisticated starting models are based on vertically converted stacking velocities. However, the resulting velocity models are strongly dependent on the initial model and the employed regularization constraints (Costa et al., 2008). Therefore, better starting models obtained by time-to-depth conversion of time-migration velocity models are highly desirable. The robustness of time migration velocity analysis indicates that such a procedure is most likely to be able to provide an high-quality alternative for the initial depth velocity model for tomography.

For these and other reasons, several attempts have been undertaken in the recent past to improve on the time-to-depth conversion of velocity models. In one line of investigation, Cameron et al. (2007, 2008) describe how to obtain depth velocity models from time migration ones using dynamic ray tracing along image rays. Their algorithm consists of image-ray tracing to convert time Dix velocities into ray coordinates

velocities and then time-to-depth convert them based on Dijkstra-like fast marching methods (Sethian, 1999a,b).

An alternative form of parameterisation of the problem was proposed by Iversen and Tygel (2008). Their technique is very similar to the previous one. The principal difference is that in the 3D case only single azimuth time migration velocity field is required as input to construct the depth velocity field. As a consequence, the image-ray transformation and its respective depth velocity field can be generated more efficiently.

While the conversion of a time migration velocity model to a depth velocity model is very attractive, its actual realization is an unstable process. Cameron et al. (2007) show the illposedness of the problem using an analytical example. Therefore, regularization is required for all algorithms trying to achieve a time-to-depth conversion of the migration velocity model. Regularization can be added in two phases: (1) during the estimation of the Dix velocity field from an estimated time migration velocity field, and (2) during the image-ray tracing.

The objective of our work is to compare three different regularization techniques for algorithms converting velocity models from time to depth. To accomplish this we apply the methods under investigation to the problem of estimating the depth velocity for the 2D Marmousoft synthetic data set (Billette et al., 2003) from a given time model. The first technique solves the problem using the algorithm of Cameron et al. (2008). Their procedure involves, besides the regularization in the Dix velocity estimation, a damped least squares velocity smoothing during the image-ray tracing. The second technique uses the algorithm described by Iversen and Tygel (2008), where regularization is built into the image-ray algorithm. In the last approach we use a modified version of the original algorithm of Cameron et al. (2007). We propose to make use of the smoothed properties of the estimated Dix velocity and a damped image-ray tracing algorithm. To evaluate the quality of the resulting depth velocity models, we compare not only the models themselves, but also the corresponding depth migrated images.

INVERSION TECHNIQUES

All of the proposed time-to-depth conversion techniques rely on the same basic idea. Their main goal is to simultaneously solve the following kinematic and dynamic ray-tracing equations given by

$$\begin{aligned}
 \frac{d\mathbf{x}}{dT} &= v^2(\mathbf{x})\mathbf{p} \\
 \frac{d\mathbf{p}}{dT} &= -\frac{1}{v(\mathbf{x})}\nabla_{\mathbf{x}}v(\mathbf{x}) \\
 \frac{\partial Q}{\partial T} &= v^2(\mathbf{x})P \\
 \frac{\partial P}{\partial T} &= \frac{-v_{nn}(\mathbf{x})}{v(\mathbf{x})}Q,
 \end{aligned} \tag{1}$$

with initial conditions

$$\begin{aligned}
 x(T=0) &= x_{0i} \\
 z(T=0) &= 0 \\
 v(x_{0i}, T=0) &= v_{Dix}(x_{0i}, T=0) \\
 Q(x_{0i}, T=0) &= 1 \\
 P(x_{0i}, T=0) &= 0.
 \end{aligned} \tag{2}$$

Here, $\mathbf{x} = (x, z)$ and \mathbf{p} are the position and slowness vectors at a point on the image ray, and x_0 is the lateral coordinate of the emergence point of the image ray. Also, T is the one-way traveltime, and Q and P are components of the propagator matrix (Červený, 2001) along the image ray. Moreover, v is the depth velocity field to be constructed in the process, and v_{nn} is its second derivative in the direction normal to the ray. In the 2D case, the velocity $v(\mathbf{x})$ is computed during the image-ray tracing from the time Dix velocity field $v_{Dix}(x_0, T)$ using the relationship

$$v(\mathbf{x}(T)) = v_{Dix}(x_0, T)Q(x_0, T), \tag{3}$$

use finite differences (FD) to solve the last two equations of system (1). Their FD scheme is

$$\begin{aligned}
 P_j^{n+1} &= \frac{P_{j+1}^n + P_{j-1}^n}{2} \\
 &\quad - \frac{\Delta T}{4\Delta x v_j^n} \left(\frac{v_{j+2}^n - v_j^n}{Q_{j+1}^n} - \frac{v_j^n - v_{j-2}^n}{Q_{j-1}^n} \right) \\
 \frac{1}{Q_j^{n+1}} &= \frac{1}{Q_j^n} - \frac{\Delta T}{2} [(V_j^n)^2 P_j^n + (V_j^{n+1})^2 P_j^{n+1}]
 \end{aligned} \tag{10}$$

where P_j^n denotes the value of P at the j th image-ray at x_{0j} and time T_n . Moreover, V_j^n denotes the Dix velocity $v_{Dix}(x_{0j}, T_n)$ in 2D and its square in 3D. In this method, no additional regularization is needed. The regularization is intrinsically performed by the P -averages that are computed in both equations of system (10). This method was inspired by the Lax-Friedrichs method for hyperbolic conservation laws (Lax, 1954), because of its total-variation diminishing property. It works because the P -averages stabilise the estimates, in this way avoiding instabilities in the FD scheme, e.g., by damping the high harmonics.

The third algorithm used in the comparisons is the one of Iversen and Tygel (2008). It first computes the derivatives $\partial v_{Dix}/\partial x_0$ and $\partial^2 v_{Dix}/\partial x_0^2$, and then updates the velocity field according to $v = v_{Dix}Q$, where x_0 is the lateral coordinate in migrated time-domain and v_{Dix} is the time Dix velocity at x_0 and T . The last step is to solve system (1), taking into account that

$$\frac{\partial v}{\partial T} = \frac{\partial v_{Dix}}{\partial T} Q + v_{Dix} \frac{\partial Q}{\partial T} \tag{11}$$

$$v_{nn} = \frac{\partial^2 v}{\partial x_0^2} + P \frac{\partial v}{\partial T}. \tag{12}$$

Equation (12) is an approximation based on the assumption that derivatives of the ray-centred coordinate q with respect to the ray position x_0 of higher order than one can be neglected. This is the only regularization of the problem included in the original algorithm of Iversen and Tygel (2008). They mention, however, that the time migration and Dix velocity models should be smooth for their algorithm to work correctly. We therefore apply the Dix velocity smoothing of equation (5) also in our realization of their algorithm.

SYNTHETIC DATA EXAMPLE

To test the three different algorithms described above, we applied them to the the Marmousoft synthetic dataset (Billette et al., 2003). First, we used the time velocity field shown in Figure 1a. However, only the technique of Cameron et al. (2008) produced acceptable results. The other techniques need a smoother input model. Therefore, applied additional smoothing to this model. All test results shown below were obtained with the smoothed version of the Marmousoft model shown in Figure 1b.

The first step of the time-to-depth conversion is the computation of the time Dix velocity field. Figure 2 compares the results of this step (a) without and (b) with regularization as described above. Note that this step is identical in all three algorithms. Although the differences are barely noticeable, the smoothing of the time Dix velocity field is essential to the tested algorithms.

Figure 3 shows the image-ray paths for all techniques. Parts a and b of Figure 3 show the results without and with Dix regularization, respectively. In the upper part of the model, there are only subtle differences between the image-ray paths resulting from the three algorithms. In the lower part, the algorithms of Cameron et al. (2008) and Iversen and Tygel (2008) produce similar results. However, there is a more visible difference between image-ray paths resulting from the proposed algorithm and the other two techniques. On the other hand, the image-ray paths in Figure 3b are a bit more similar to each other, particularly in the lateral direction. This was to be expected because of the additional smoothing regularization in the Dix velocity computation.

Figure 4 shows the depth velocity fields as obtained using the three algorithms applied to the Dix velocity field without the additional regularization step, and Figure 5 shows their correspondent prestack depth migrated sections. In both figures, parts (a) to (c) refer to the algorithms in the following order: (a) the one proposed here, (b) the one of Cameron et al. (2008), and (c) the one of Iversen and Tygel (2008). We

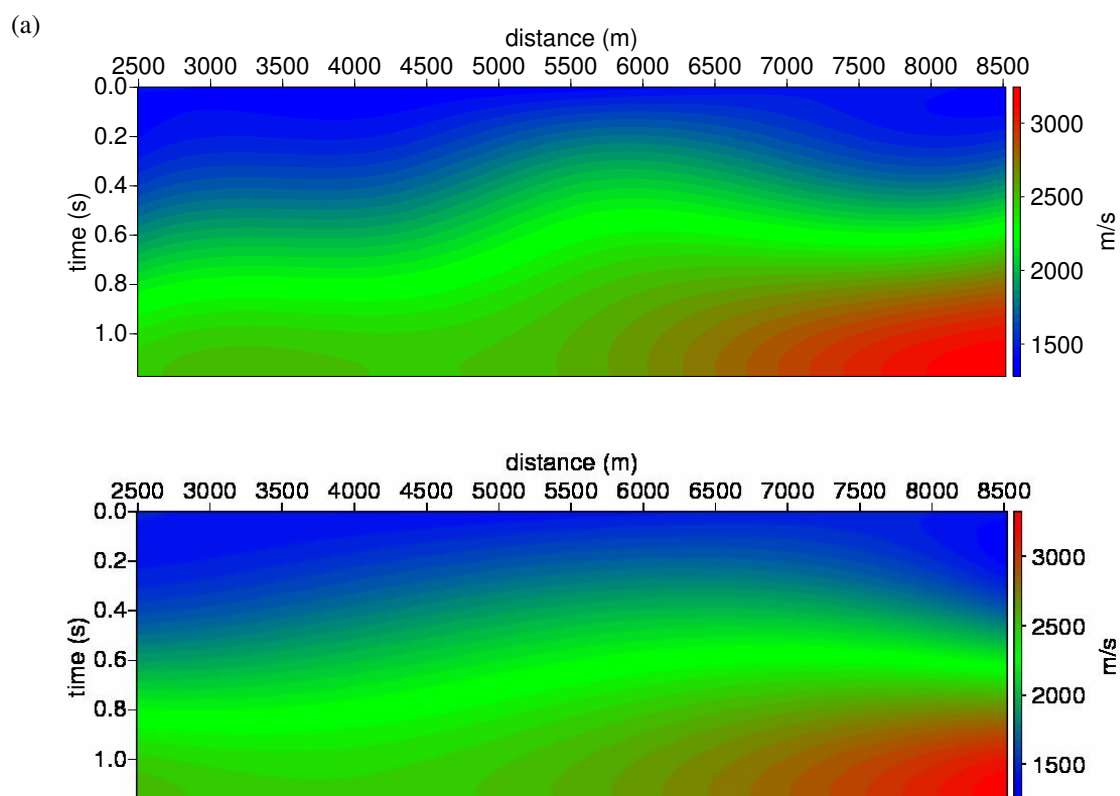


Figure 1: (a) Time migration velocity of Marmousoft; (b) Smoothed time migration velocity of Marmousoft.

see some differences between the obtained depth velocity fields in Figure 4. For example, the algorithm of Cameron et al. (2008) yields the lowest velocity values in the high velocity zone in the bottom right corner. On the other hand, the algorithm of Iversen and Tygel (2008) produces the most pronounced low-velocity zone in the bottom left corner. Other, less prominent differences are also visible, like the slight shift in the lateral position of the lower velocities at about 2000 m depth or the slightly different depths of the lower velocities at the top of the model.

In spite of these rather strong differences between the velocity models, the resulting prestack migrated images in Figure 5 look very similar, indicating that probably all of the algorithms provide good starting models for a subsequent tomographic analysis. The image obtained with the velocity model from our proposed algorithm (Figure 5a) seems to provide slightly better focus than the other images in the bottom right corner, while the image obtained with the algorithm of Cameron et al. (2008) seems slightly superior in the bottom left corner. All conversions seem to do quite a good job in the lateral parts of the model, while running into difficulties in the more complex centre part. Of course, the reason for this behaviour is the inadequacy of time migration in this rather complex area, indicating that this is not a problem of the conversion algorithms but of the original time-migration velocity model.

The final sets of Figures 6 and 7 show the results of time-to-depth velocity conversion and the corresponding prestack depth migrated images when regularization according to equation (5) is applied to the Dix velocities. The figure parts show the results from the different algorithms in the same order as before. The differences between the individual results are to great extent the same as before. On the other hand, the differences between the velocity models without and with Dix regularization (compare Figures 4 and 6) are barely visible. Therefore, it comes as quite a surprise that the very subtle differences between those models lead to significant differences in the resulting migrated images (compare Figures 5 and 7). While the images in Figure 7 again do not differ much from one another, the differences to the images in Figure 5 are more obvious. It is clearly visible that many of the instabilities in the images of Figure 5 are gone in

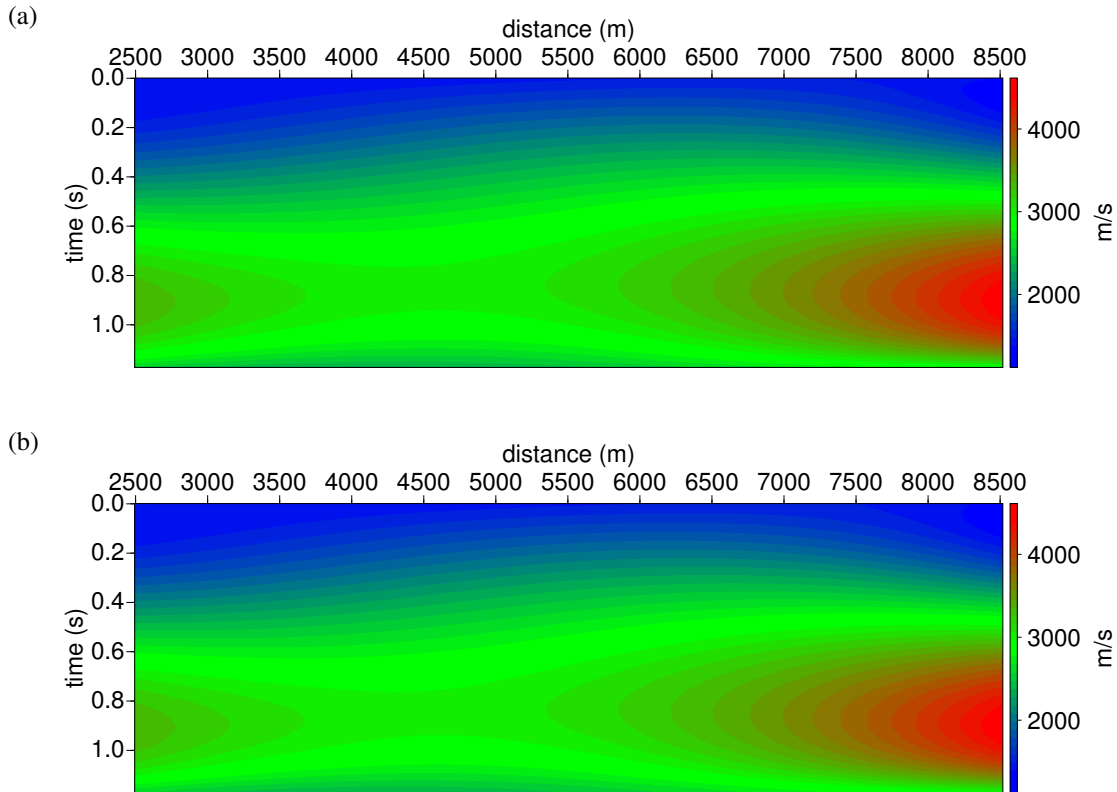


Figure 2: Time Dix velocity from the smoothed time migration velocity of Marmousoft (a) without regularization; (b) with regularization with $\alpha = 0.01$.

Figure 7.

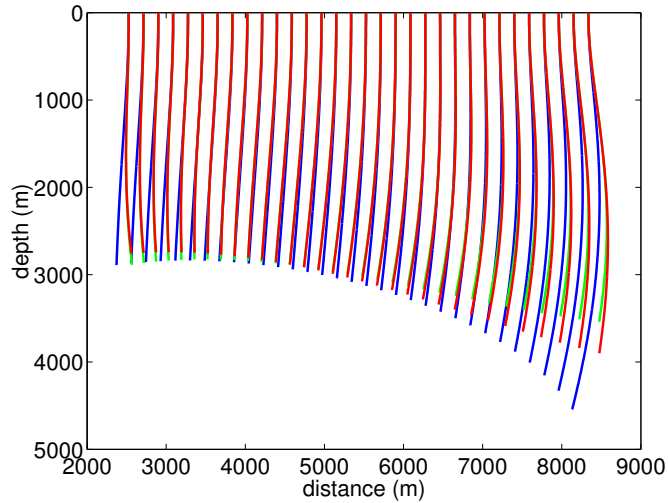
We conclude from our numerical examples that the actual choice of the algorithm to solve system (1) most strongly affects the resulting model. It does not seem to make much of a difference with respect to the final migrated image. For this reason, we expect it to also make no difference when using the obtained models as starting models for tomographic velocity analysis. On the other hand, independently of the chosen algorithm, the addition of the Dix velocity regularization in the process helps to stabilise the migrated images. Therefore this regularization is probably also to be recommended for tomography purposes.

CONCLUSIONS

Since time migration velocity analysis is a mature and robust technology, time-to-depth conversion of a velocity model is highly desirable. Such converted velocity models can then be an input to velocity refinement techniques like depth migration velocity analysis or tomographic methods. Unfortunately, the problem of converting a time velocity model to depth is intrinsically unstable and thus requires regularization. Recently, a number of similar techniques using dynamic ray tracing along image-rays have been proposed to achieve this aim.

In this work, we have compared three different algorithms to estimate a depth velocity model from a time migration velocity model. All these algorithms are variations of the original algorithm presented by Cameron et al. (2007). Due the ill-posed nature of this problem, the different ways how the different algorithms handle regularization determine the results. The algorithm of Cameron et al. (2008) only relies on intrinsic regularization embedded in the employed Lax-Friedrichs FD scheme. The algorithm of Iversen and Tygel (2008) merely neglects a second derivative. Moreover, it assumes the input Dix velocity to be sufficiently smooth to avoid instabilities or the occurrence of caustics during the image-ray tracing. We

(a)



(b)

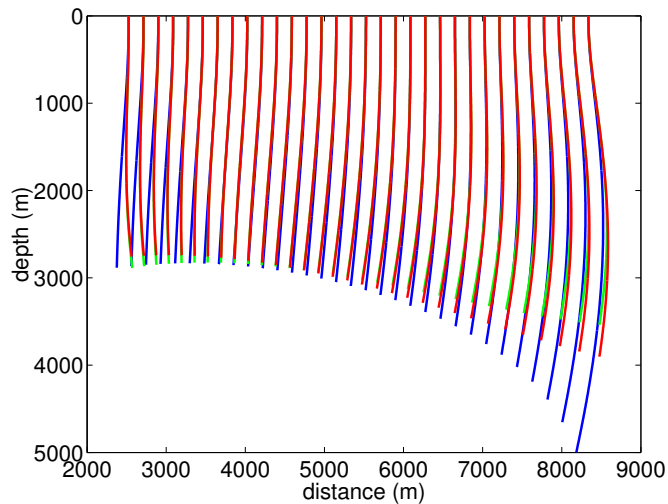


Figure 3: Image-ray paths using the v_{Dix} velocity field with parameters $p = 5$ and $\beta = 0.05$. Blue rays correspond to the proposed algorithm, green ones to Cameron et al. (2008), and red ones to Iversen and Tygel (2008). (a) Dix model without regularization; (b) Dix model with regularization with $\alpha = 0.01$.

have compared these algorithms to a modified version of the original algorithm presented by Cameron et al. (2007), in which we propose to add a smoothing of the image-ray wavefront during the image-ray tracing to improve stability. Based on our experiences with synthetic experiments, we propose to add to all algorithms an additional regularization step in the calculation of the Dix velocity model from the original time migration velocities.

To test the discussed algorithms numerically, we have applied all three of them to a time-migration velocity model from the Marmousfit synthetic dataset. Our numerical experiments indicate that both levels of regularization are required. A smooth Dix velocity model is crucial for algorithms that do not smooth the image front during the ray-tracing, as occurs in the direct implementation of the algorithm proposed by Iversen and Tygel (2008), or even the algorithm proposed by Cameron et al. (2008). Our proposed additional regularization of the image wavefront during the image-ray tracing reduces the dependency on the initial Dix velocity field, in this way making the algorithm more robust. The particular form of smoothing we have chosen reduces the dependency of the algorithm on the degree of the polynomial used to fit the image front.

The depth velocity models estimated in our numerical examples indicate the effects of the different

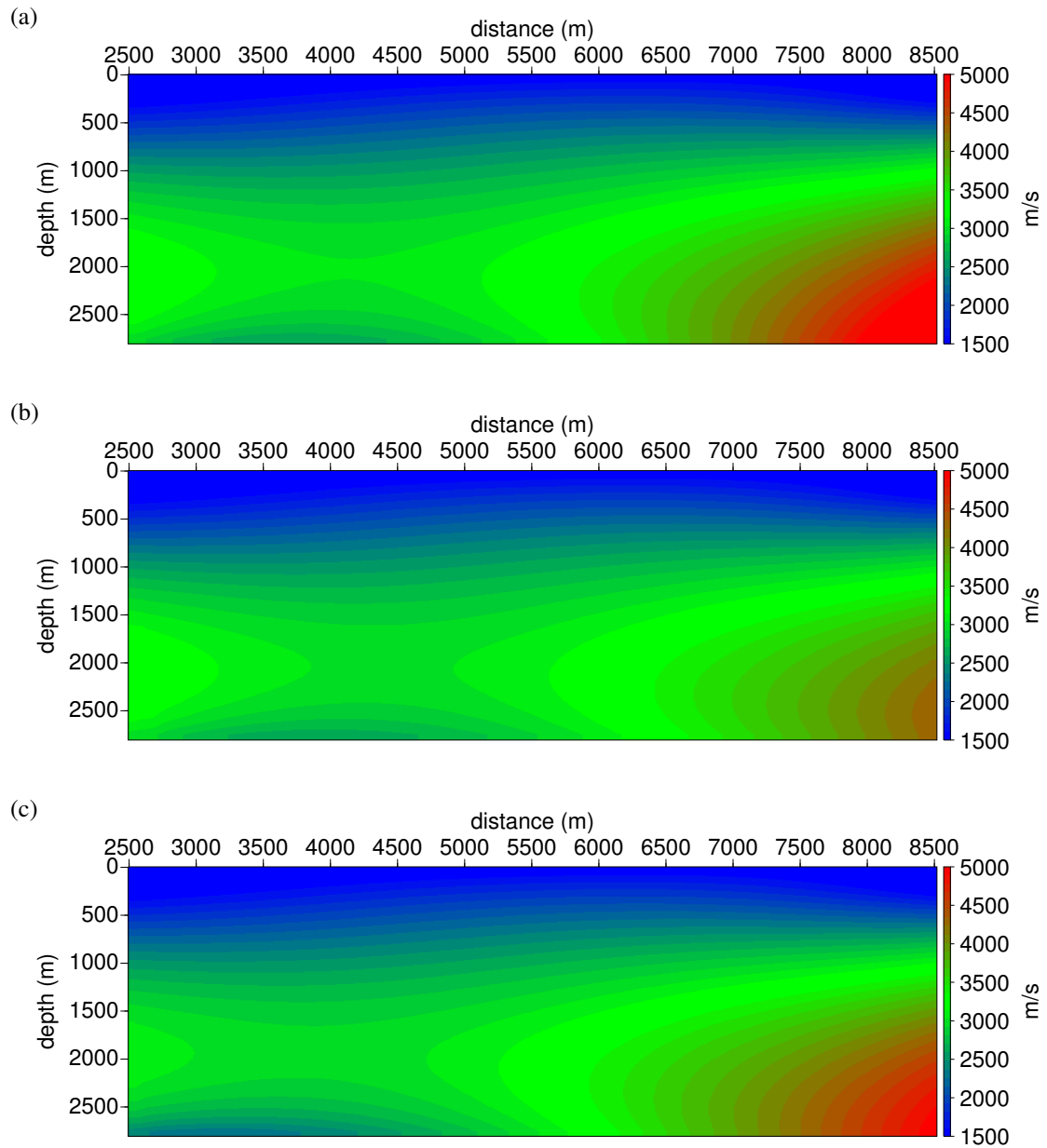


Figure 4: Depth velocity model obtained from time velocity model without Dix regularization and $p = 5$, $\beta = 0.05$. (a) Proposed algorithm; (b) Cameron et al. (2008) algorithm; (c) Iversen and Tygel (2008) algorithm.

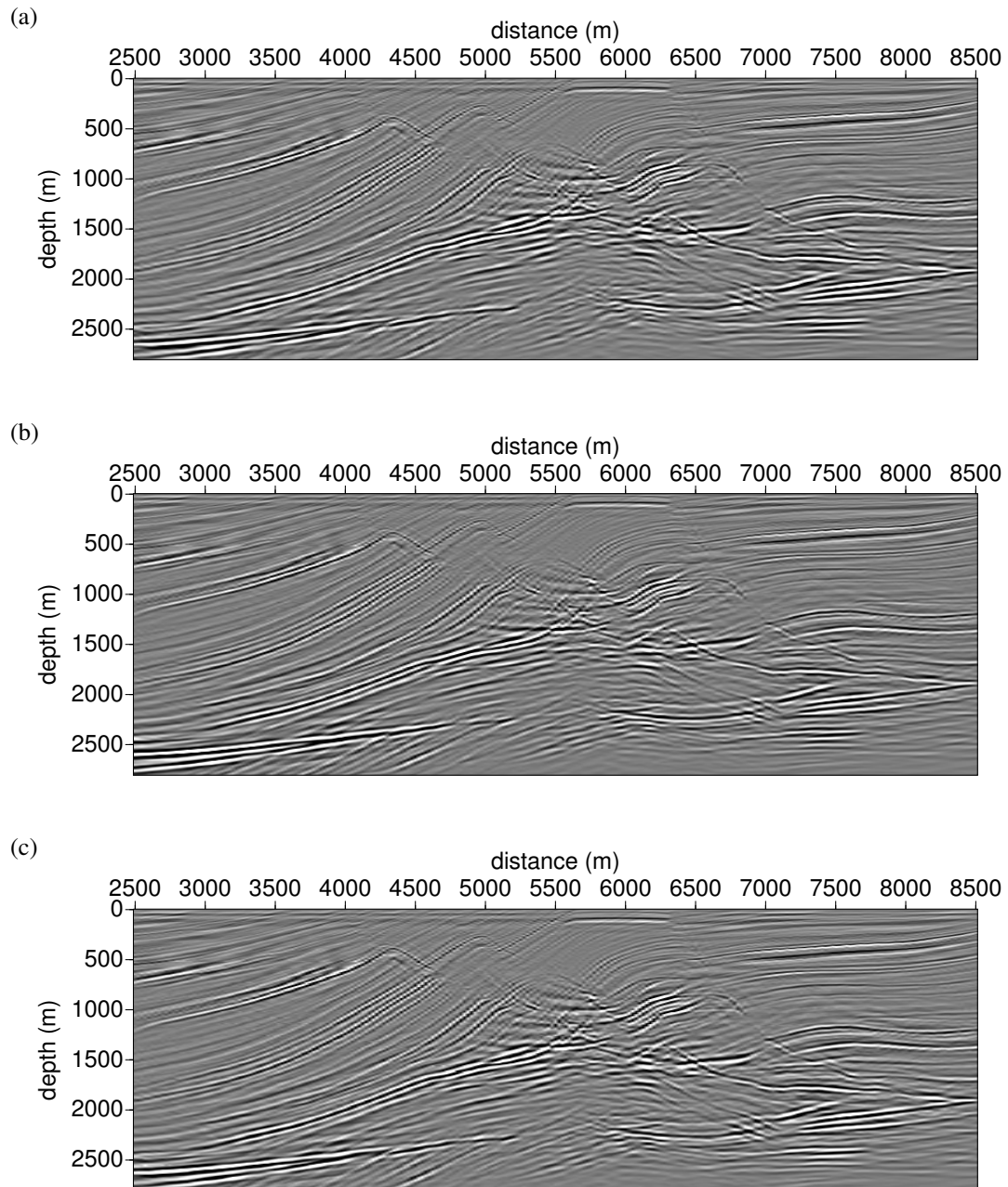


Figure 5: Prestack depth migrated sections obtained from depth velocity models of Figure 4.

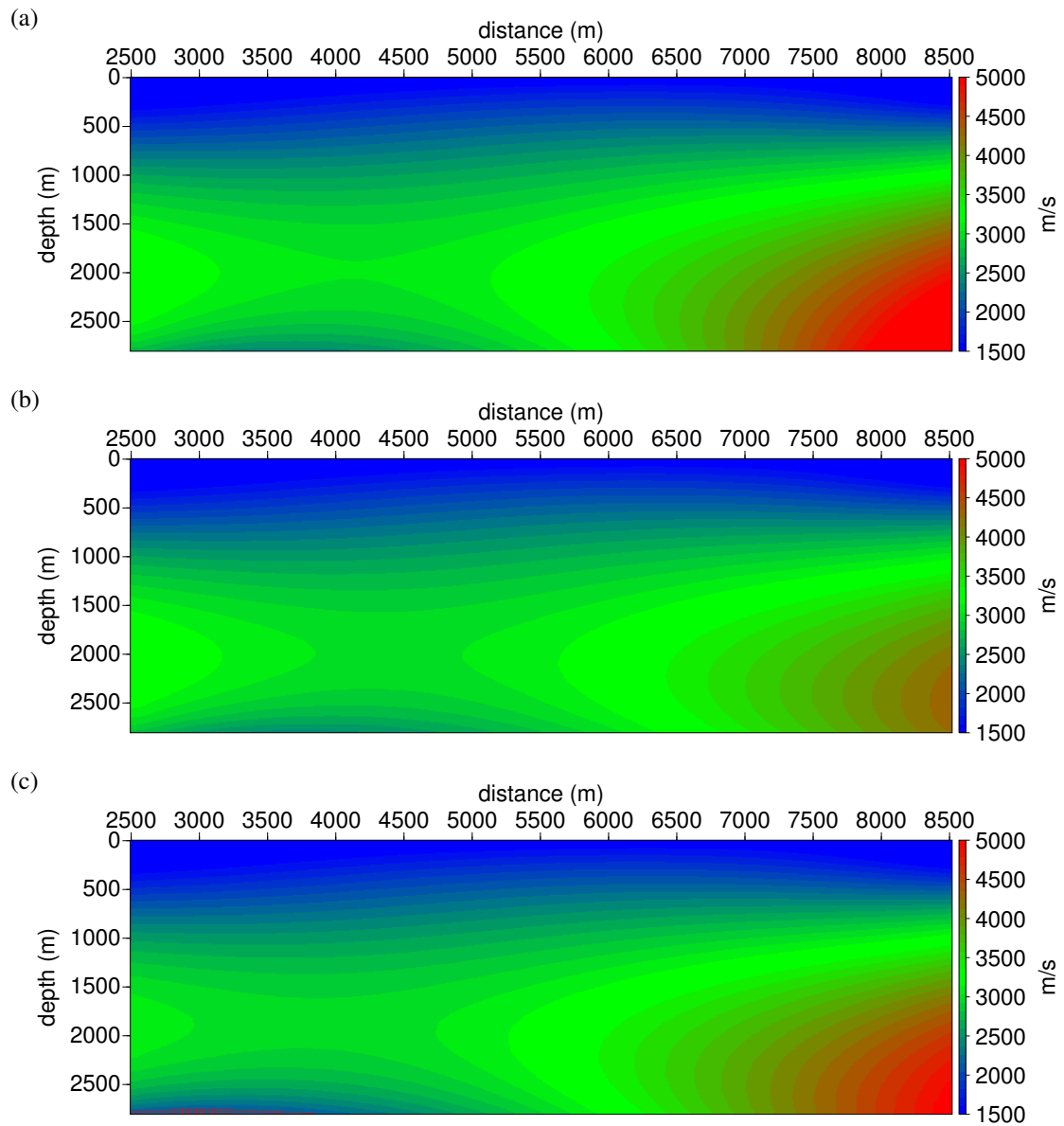


Figure 6: Depth velocity models obtained from time-to-depth conversion with Dix regularization using $p = 5$, $\alpha = 0.01$, and $\beta = 0.05$. (a) Proposed algorithm; (b) algorithm of Cameron et al. (2008); (c) algorithm of Iversen and Tygel (2008).

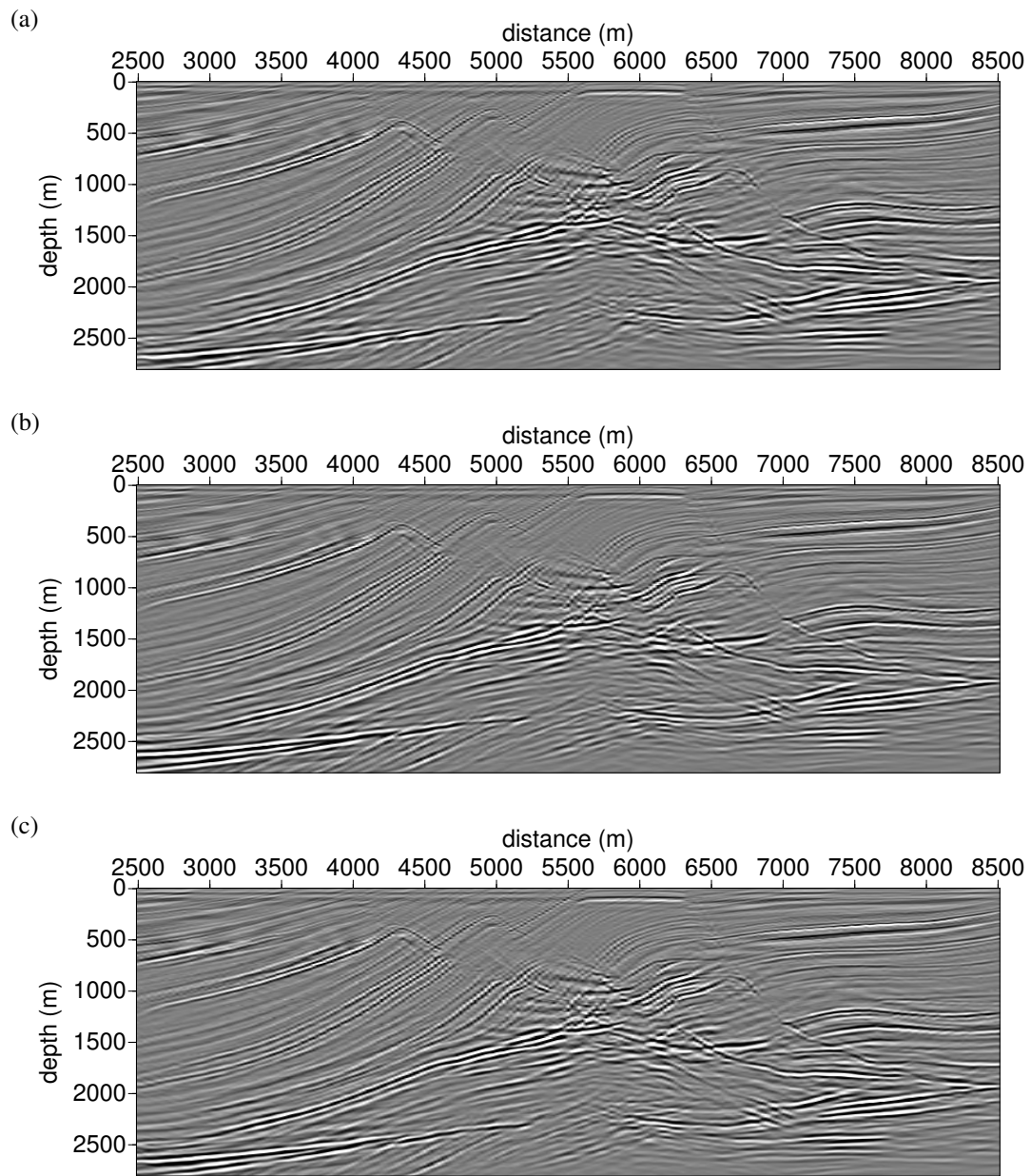


Figure 7: Prestack depth migrated sections obtained from depth velocity models of Figure 6.

regularization strategies. These effects are the most evident when looking at the image-ray trajectories. In the shallow part of the model these trajectories are almost coincident, because of the small lateral variation of the input Dix velocity field. In the bottom part of the model, where the lateral velocity variation is stronger, the image-ray trajectories differ for each algorithm. The additional smoothing of the input Dix velocity field helps to reduce these differences.

The difference in the image-ray paths leads to differences in the converted velocity models. Our numerical tests indicate that these model difference do not have a strong impact on the depth migrated images. It remains to be seen whether these differences have important consequences when these models are used as the initial models for tomography. Another important observation concerns the Dix velocity smoothing during the image-ray tracing. While this smoothing does not seem to significantly influence the resulting depth velocity models, it has shown a beneficial impact on the depth migrated images, strongly reducing instabilities and thus making the image less noisy. Future research will have to show whether the Dix velocity smoothing also has a beneficial impact on the tomographic velocity updates.

ACKNOWLEDGEMENTS

We acknowledge CAPES, CNPq, FINEP, PETROBRAS and ANP for financial support. This work was kindly supported by the sponsors of the *Wave Inversion Technology (WIT) Consortium*, Karlsruhe, Germany.

REFERENCES

- Billette, F., Le Bégat, S., Podvin, P., and Lambaré, G. (2003). Practical aspects and applications of 2D stereotomography. *Geophysics*, 68(3):1008–1021.
- Cameron, M. K., Fomel, and Sethian, J. A. (2008). Time-to-depth conversion and seismic velocity estimation using time-migration velocity. *Geophysics*, 73(5):VE205–VE210.
- Cameron, M. K., Fomel, S. B., and Sethian, J. A. (2007). Seismic velocity estimation from time migration. *Inversion Problems*, 23:1329–1369.
- Červeny, V. (2001). *Seismic ray theory*. Cambridge University Press, Cambridge.
- Clapp, R. G., Biondi, B., and Claerbout, J. F. (2004). Incorporating geologic information into reflection tomography. *Geophysics*, 69(2):533–546.
- Costa, J. C., Silva, F. C. J., Gomes, E. N. S., Schleicher, J., Melo, L. A. V., and Amazonas, D. (2008). Regularization in slope tomography. *Geophysics*, 73(5):VE39–VE47.
- Fomel, S. (2003). Time migration velocity analysis by velocity continuation. *Geophysics*, 68(5):1662–1672.
- Iversen, E. and Tygel, M. (2008). Image-ray tracing for joint 3d seismic velocity estimation and time-to-depth conversion. *Geophysics*, 73(3):S99–S114.
- Lax, P. D. (1954). Weak solutions of hyperbolic equations and their numerical computation. *Communications in Pure and Applied Mathematics*, 7:159–193.
- Schleicher, J. and Costa, J. C. (2009). Migration velocity analysis by double path-integral migration. *Geophysics*, page in review.
- Schleicher, J., Costa, J. C., and Novais, A. (2008). Time-migration velocity analysis by image-wave propagation of common image-gathers. *Geophysics*, 73(5):VE161–VE171.
- Sethian, J. A. (1999a). Fast marching methods. *SIAM Review*, 41(2):199–235.
- Sethian, J. A. (1999b). *Level set methods and fast marching methods*. Cambridge University Press, Cambridge.
- Valente, L. S. S. (2007). Velocity model estimation in depth from time-migration velocities. Course completion assignment, Federal University of Pará. In Portuguese.